AGU PUBLICATIONS

JGR

Journal of Geophysical Research: Space Physics

RESEARCH ARTICLE

10.1002/2014JA019891

Key Points:
- New paradigm for origin of Jupiter's radiation belts
- Chorus waves drive a very large increase in electron flux from a soft spectrum
- Radial diffusion transports electrons inward at $L < 9$ and outward for $L > 9$

Correspondence to:
E. E. Woodfield,
emmwoo@bas.ac.uk

Citation:
Woodfield, E. E., R. B. Horne, S. A. Glauert, J. D. Menietti, and Y. Y. Shprits (2014), The origin of Jupiter's outer radiation belt, *J. Geophys. Res. Space Physics*, *119*, 3490–3502, doi:10.1002/2014JA019891.

Received 14 FEB 2014
Accepted 19 APR 2014
Accepted article online 24 APR 2014
Published online 15 MAY 2014

The origin of Jupiter's outer radiation belt

E. E. Woodfield[1], R. B. Horne[1], S. A. Glauert[1], J. D. Menietti[2], and Y. Y. Shprits[3,4,5]

[1]British Antarctic Survey, Cambridge, UK, [2]Department of Physics and Astronomy, University of Iowa, Iowa City, Iowa, USA, [3]Skolkovo Institute of Science and Technology, Moscow, Russia, [4]Massachusetts Institute of Technology, Cambridge, Massachusetts, USA, [5]University of California, Los Angeles, California, USA

Abstract The intense inner radiation belt at Jupiter (>50 MeV at 1.5 R_J) is generally accepted to be created by radial diffusion of electrons from further away from the planet. However, this requires a source with energies that exceed 1 MeV outside the orbit of the moon Io at 5.9 R_J, which has never been explained satisfactorily. Here we test the hypothesis that this source population could be formed from a very soft energy spectrum, by particle injection processes and resonant electron acceleration via whistler mode chorus waves. We use the British Antarctic Survey Radiation Belt Model to calculate the change in the electron flux between 6.5 and 15 R_J; these are the first simulations at Jupiter combining wave particle interactions and radial diffusion. The resulting electron flux at 100 keV and 1 MeV lies very close to the Galileo Interim Radiation Electron model spectrum after 1 and 10 days, respectively. The primary driver for the increase in the flux is cyclotron resonant acceleration by chorus waves. A peak in phase space density forms such that inside $L \approx 9$ radial diffusion transports electrons toward Jupiter, but outside $L \approx 9$ radial diffusion acts away from the planet. The results are insensitive to the softness of the initial energy spectrum but do depend on the value of the flux at the minimum energy boundary. We conclude by suggesting that the source population for the inner radiation belt at Jupiter could indeed be formed by wave-particle interactions.

1. Introduction

Jupiter has extremely intense radiation belts which generate synchrotron radiation from highly relativistic electrons [*Bolton et al.*, 2002; *de Pater and Dunn*, 2003]. The formation of these belts can be described by radial diffusion of electrons originating outside the orbit of the moon Io [*Santos-Costa and Bourdarie*, 2001; *Sicard and Bourdarie*, 2004]. This motion increases the energy of the electrons since the first adiabatic invariant is conserved. Figure 1 shows the increase in electron energy for constant first invariant, μ, assuming a dipole magnetic field at Jupiter. There is a long history of modeling the inner Jovian radiation belts ($L < 5$) using radial diffusion [*de Pater and Goertz*, 1990; *Santos-Costa and Bourdarie*, 2001; *de Pater et al.*, 2003; *Sicard and Bourdarie*, 2004], much of which involves comparison with the synchrotron radiation emission from Jupiter that has been measured by terrestrial radio telescopes for several decades [e.g., *Berge and Gulkis*, 1976; *Sault et al.*, 1997; *de Pater and Dunn*, 2003]. In order for this radial transport to successfully create the very intense inner radiation belt (>50 MeV), a suitable source of electrons with energies of approximately 1 MeV is required at approximately 10 R_J.

Until recently, there was no explanation for the presence of this "seed" population outside of the moon Io. There are dynamic processes in the region outside of Io which bring hotter electrons inward in bursts. Interchange events such as that described in *Thorne et al.* [1997] bring more energetic electrons inward by a relatively small distance ($L = 6.3$ to 6.03) and have an energy of tens of keV. Other injections in this region are in the range from tens of keV to hundreds of keV [*Mauk et al.*, 1999; *Louarn et al.*, 2001]. However, neither of these processes bring in sufficiently energetic electrons to be radially diffused up to 50 MeV in the inner radiation belt. Therefore, there must be local acceleration present.

Horne et al. [2008] suggested the idea that wave particle interactions may be the source of the local acceleration which accelerates the existing population of electrons beyond Io to the right energies to become the ultrarelativistic inner radiation belt. At the Earth, chorus waves are very effective at accelerating electrons [*Summers et al.*, 1998; *Horne et al.*, 2005; *Chen et al.*, 2007]. Intense chorus waves have also been observed at Jupiter [e.g., *Menietti et al.*, 2008, 2012], an example of which is shown in Figure 2. Jovian whistler mode chorus is believed to be generated by the inward motion of relatively warm electrons resulting from the interchange instability [*Thorne et al.*, 1997], which in turn cause a temperature anisotropy with free energy

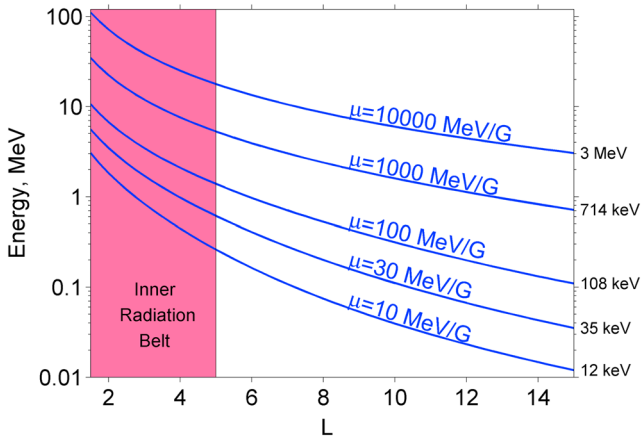

Figure 1. Electron energy as a function of L for constant first adiabatic invariant, μ, assuming a dipole magnetic field at Jupiter.

for the waves to grow. The hypothesis that wave-particle interactions, specifically with whistler mode chorus, are responsible for the source of the inner radiation belts was later expanded on by *Shprits et al.* [2012] and *Woodfield et al.* [2013].

The injections investigated by *Mauk et al.* [1999] and *Louarn et al.* [2001] are thought to be more similar to substorm injections at Earth than the interchange events (although the generating source of these "storm-like" injections at Jupiter is far from clear). The time-dispersed dynamic injections surveyed in *Mauk et al.* [1999] have no longitude or local time dependence but show a peak occurrence near $L = 10$ to 12. The characteristic time of these injections is 1 h. Whether these injections are related to the interchange instability or not remain unclear, although *Russell et al.* [2004] suggest that the events reported in *Mauk et al.* [1999] may be caused by the irregular outflow of mass from Io. Given the location and energy range of these dynamic injections, they are an ideal candidate to drive generation of whistler mode chorus which in turn can accelerate electrons to the energies observed in the outer radiation belt.

In this paper we hypothesize that the electrons injected during the events described by *Mauk et al.* [1999] are accelerated by whistler mode chorus waves to the energies necessary to create the inner radiation belts at Jupiter. We perform simulations using the British Antarctic Survey (BAS) radiation belt model adapted to Jupiter (hereafter referred to as the BAS model [*Glauert et al.*, 2014]) to investigate this idea. To the best of our knowledge, these are the first radiation belt simulations at Jupiter to include both wave-particle interactions and radial diffusion.

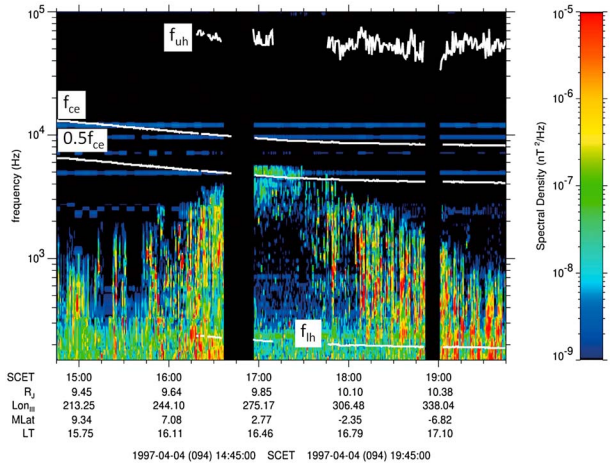

Figure 2. An example of wave activity at Jupiter from the Galileo spacecraft. The four labeled white lines are the upper hybrid frequency, f_{uh}, the electron gyrofrequency, f_{ce}, $0.5f_{ce}$, and the maximum lower hybrid frequency, f_{lh}. The band of wave power near 1700 spacecraft event time at approximately 5 kHz corresponds to upper band chorus waves. The band of waves just below at about 3–4 kHz corresponds to lower band chorus. Note that the emissions appear as short bursts of intense waves. The horizontal lines are interference from the spacecraft.

2. BAS Radiation Belt Model at Jupiter

The BAS model uses quasi-linear theory to model planetary radiation belts using a diffusion equation [*Glauert et al.*, 2014] and a fixed, average wave spectrum. Quasi-linear theory has been extensively used in radiation belt modeling at the Earth [e.g., *Varotsou et al.*, 2005, 2008; *Albert et al.*, 2009; *Shprits et al.*, 2009a, 2009b; *Fok et al.*, 2008; *Su et al.*, 2010; *Glauert et al.*, 2014] and has also been applied at Jupiter [*Horne et al.*, 2008; *Shprits et al.*, 2012; *Woodfield et al.*, 2013]. It is well known that nonlinear effects are important for the generation of chorus waves [e.g., *Trakhtengerts*, 1999; *Nunn et al.*, 1997; *Omura et al.*, 2009]; however, simulating chorus waves using nonlinear theory over the time and spatial scales required for global modeling of radiation belts is not yet computationally feasible. Comparisons between particle scattering in the fully nonlinear and diffusive regimes [*Albert*, 2010]

and test particle simulations [*Tao et al.*, 2012] show a remarkable agreement for small-amplitude waves. We therefore adopt the well-accepted approximation of quasi-linear theory, which assumes a broad band of small-amplitude, uncorrelated waves and uses the time-averaged wave power (neglecting the phase trapping of the electrons). This method also includes the assumption that the average wave spectrum used in the calculations is unaltered by the resonant interaction of the waves and particles.

The BAS model uses an unconditionally stable fully implicit numerical scheme to solve the modified Fokker-Planck equation at Jupiter [*Glauert et al.*, 2014; *Shprits et al.*, 2009b] given by

$$\frac{\partial f}{\partial t} = \frac{1}{g(\alpha)} \left.\frac{\partial}{\partial \alpha}\right|_{E,L} \left(g(\alpha) D_{\alpha\alpha} \left.\frac{\partial f}{\partial \alpha}\right|_{E,L} \right) + \frac{1}{A(E)} \left.\frac{\partial}{\partial E}\right|_{\alpha,L} \left(A(E) D_{EE} \left.\frac{\partial f}{\partial E}\right|_{\alpha,L} \right) + L^2 \left.\frac{\partial}{\partial L}\right|_{\mu,J} \left(\frac{1}{L^2} D_{LL} \left.\frac{\partial f}{\partial L}\right|_{\mu,J} \right) - \frac{f}{\tau} \quad (1)$$

where

$$g(\alpha) = \sin 2\alpha \left(1.3802 - 0.3198 \left(\sin\alpha + (\sin\alpha)^{\frac{1}{2}} \right) \right) \quad (2)$$

$$A(E) = (E + E_0) \left(E(E + 2E_o) \right)^{\frac{1}{2}} \quad (3)$$

where f is the phase space density, α is the equatorial pitch angle, $D_{\alpha\alpha}$, D_{EE}, and D_{LL} are the drift- and bounce-averaged pitch angle, energy, and radial diffusion coefficients, respectively, E_0 is the electron rest energy, and τ is the loss timescale (infinite outside the loss cone and 1/4 of the bounce time inside). The model uses a two-grid method where solutions for the pitch angle and energy diffusion are sought on a grid in pitch angle, energy, and L (α, E, L) and for the radial diffusion on a (μ, J, L) grid, where μ and J are the first and second adiabatic invariants, respectively. The grids are interpolated using cubic splines as described in *Glauert et al.* [2014]. We use a grid of 90 points in α and 30 each in L and energy. The loss cone angle is set to a fixed value of 2.1° in our simulation for Jupiter corresponding to the loss cone angle at $L = 10$. This will result in an overestimate of losses at $L > 10$ and an underestimate of the losses at $L < 10$, if we were to set the change to collisional-dominated atmosphere at 1.3 R_J [*Wang et al.*, 2002]. The four terms of equation (1) represent diffusion in pitch angle, diffusion in energy, radial diffusion, and finally losses to the atmosphere. The pitch angle and energy diffusion coefficients are calculated separately before solving equation (1) using the PADIE code (Pitch Angle and energy Diffusion of Ions and Electrons [*Glauert and Horne*, 2005]) to generate a value of $D_{\alpha\alpha}$ and D_{EE} for each electron energy, pitch angle, and L shell. We then assume that the underlying cold plasma conditions on which $D_{\alpha\alpha}$ and D_{EE} are based do not change while solving equation (1) over time.

In the full derivation of equation (1) there are derivatives involving both pitch angle and energy in the same term; these cross diffusion terms are not included in the BAS model. The cross terms tend to inhibit acceleration; however, *Tao et al.* [2009] found that at Earth for pitch angles close to 90°, the cross terms have a limited effect on the acceleration, but at energies of a few MeV and low pitch angles the flux can be significantly overestimated without the cross terms. Our results focus on the pitch angles near to 90°, so we do not expect the lack of cross terms to have a particularly large effect.

The chorus waves in our simulations are assumed to be field aligned. *Tao et al.* [2011] show that using a varying wave normal angle with latitude, based on calculations for Jupiter from the HOTRAY ray tracing program [*Horne*, 1989], results in a smaller increase in the flux after 30 days. The flux after 30 days is smaller by a factor of between 1.1 and 7 for 1 to 10 MeV electrons at pitch angles greater than 20° compared to field-aligned simulations [*Tao et al.*, 2011, Figure 11]. This factor is small in comparison to the flux increases we will show in the following sections and will therefore be neglected.

We have used a dipole model of Jupiter's magnetic field and have therefore deliberately restricted the range of L values over which we run the model to $L < 15$. According to *Tomás et al.* [2004], the change from dipole-dominated magnetic field to current sheet-dominated field occurs between 12 and 20 R_J. We have used the low-energy plasma density model of *Bagenal* [1994].

We use an initial pitch angle distribution of the phase space density equal to $\sin(\alpha)$ multiplied by the phase space density at $\alpha = 90°$. The steepness of the initial pitch angle distribution is not critical to the model results in our simulations; for example, using a factor of $\sin^3(\alpha)$ produces almost identical results after only a short simulation time. At the edges of the pitch angle grid ($\alpha = 0°, 90°$) we set the gradient of phase space density with pitch angle to zero. The constant flux values for the minimum energy boundary (20 keV

at $L = 15$) are taken from an approximation to the Galileo Interim Radiation Environment model (GIRE) [*Garrett et al.*, 2003]. This empirical model fits a functional form to the Galileo energetic particle data and is valid from $L = 8.25$ to 16.25. To provide a very simple extension of this model close to the orbit of Io, we have fitted a power law to each of the four variables in the GIRE model which we then use to extrapolate from $L = 8.25$ to $L = 6.5$. At the maximum energy boundary (25 MeV at $L = 15$) we use a constant, very low value for the flux of 10^{-4} cm^{-2} s^{-1} sr^{-1} keV^{-1} which is approximately the lowest flux of any energy in the GIRE model at $L = 15$.

The radial diffusion of electrons at Jupiter is thought to be caused by ionospheric dynamo winds as suggested by *Brice and McDonough* [1973], whereas at the Earth, radial diffusion is driven via ultralow frequency waves and fluctuations in the large-scale electrostatic fields [*Brautigam and Albert*, 2000]. Radial diffusion proceeds by fluctuations in the third adiabatic invariant which are more rapid than a trapped particle's drift period, while conserving the first and second adiabatic invariants. This is possible because the gyration and bounce periods associated with the first and second invariants are much shorter than the drift period. The conservation of the first invariant leads to the increase (decrease) of the energy of the particles as they diffuse inward (outward) as shown in Figure 1. The energy input to drive the diffusion comes from the source of the fluctuations, at Jupiter, this is ultimately due to the rotation of the planet. Radial diffusion rates are usually expressed as

$$D_{LL} = D_0 L^n \tag{4}$$

where D_0 is a scaling factor and L is the L shell number. At Earth the power law scaling value, n, is typically in the range $6 < n < 10$ [*Schulz and Lanzerotti*, 1974]. At Jupiter, $n = 3$ following *Brice and McDonough* [1973]. *de Pater and Goertz* [1994] performed an extensive study on radial diffusion at Jupiter based on synchrotron radiation observations and found that $D_0 = 3 \times 10^{-9}$ s^{-1} resulting in much longer diffusion rates than at Earth. This is the value of D_0 we use in our calculations.

2.1. Diffusion Rates From Chorus

Injections of higher-energy electrons into the existing lower-energy population create excellent conditions for the growth of whistler mode chorus waves through a temperature anisotropy with free energy available for the waves to grow. Evidence for chorus wave growth coincident with injections at the Earth has been reported by, e.g., *Horne et al.* [2003] and *Li et al.* [2009]. At Jupiter, the same mechanism is also thought to occur, for example, in the presence of interchange events [*Xiao et al.*, 2003]. It is therefore reasonable to assume that the *Mauk et al.* [1999] injections will also generate whistler mode chorus waves.

The diffusion rates we use for chorus in this paper are identical to those used in *Woodfield et al.* [2013]. These authors fitted a Gaussian profile to wave data from the Galileo spacecraft to create an empirical model of the variation of chorus power with latitude and radial distance at Jupiter; this extrapolates the data to $\gtrsim 10°$ magnetic latitude where there is no Galileo data. There is a peak in the chorus intensity near $L = 9$, and the intensity increases slightly with magnetic latitude to about 5° and then drops significantly by 20°. In this paper we include all wave power up to 30°. The diffusion rates were calculated using the PADIE code [*Glauert and Horne*, 2005] and were averaged along the path of the electrons over a bounce period (we denote the bounce averaged diffusion rates as $< D_{EE} >$ and $< D_{\alpha\alpha} >$). The input parameters used in our calculations are shown in Table 1 where a Gaussian power spectrum is assumed for the chorus wave frequency.

Figure 3 shows how our values for pitch angle and energy diffusion rates compare to radial diffusion timescales at Jupiter for 0.1 MeV and 1 MeV electrons (Figures 3a and 3b, respectively). In order to present all the diffusion rates with the same units of d^{-1}, we show $< D_{EE} > /E^2$ rather than $< D_{EE} >$ [see *Glauert and Horne*, 2005]. It is important to recall that while $< D_{\alpha\alpha} >$ and $< D_{EE} >$ depend on pitch angle, energy, and L value, D_{LL} depends only on L; therefore, the values of D_{LL} do not change between the two panels. Figure 3 shows that at 0.1 MeV pitch angle diffusion dominates and is significantly greater than D_{LL} at all the L values shown here. However, at 1 MeV the energy diffusion rate is greater than pitch angle diffusion rate and comparable to the rate of radial diffusion. This indicates that an injection of electrons at energies of the order of a few tens of keV to a few hundred keV like those discussed in *Mauk et al.* [1999] will be subject to rapid acceleration in the presence of the chorus waves since the product of the energy diffusion coefficient and the phase space density gradient in energy (second term of equation (1)) should be large.

Table 1. Inputs to the PADIE Code Used in This Paper

PADIE Input	Value
Peak frequency	$0.15f_{ce}$
Frequency width	$0.05f_{ce}$
Peak wave normal angle, ψ	0°
Wave normal angle distribution	$\chi = \tan(\psi)$
Width of χ	$\chi_w = \tan(30°)$
Cyclotron harmonic resonances used	$n = 0, \pm1, \pm2, \pm3, \pm4, \pm5$
Plasma density model	*Bagenal* [1994]
Magnetic field model	Dipole, $B_{equator} = 409\,\mu T$

We also include in our calculations a contribution to pitch angle diffusion from collisions with the atmosphere. This only affects electrons close to and inside the loss cone where collisions cause rapid loss of electrons to the atmosphere. The loss cone is a very sharp and somewhat unrealistic boundary defined using one altitude where all particles are assumed to be lost (in our simulations this loss altitude changes with L because we are using a fixed loss cone angle). In reality, losses due to collisions with the atmosphere will start above the loss altitude, although the probability of a collision will be lower. The inclusion of diffusion due to collisions effectively smears out this unrealistically sharp boundary at the loss altitude by rapidly scattering electrons close to, but just outside the loss cone into the region of the model where they are lost according to the fourth term of equation (1). This contribution to the overall pitch angle diffusion rates can be seen in Figure 4a as the steep increase in $< D_{\alpha\alpha} >$ at very low pitch angle. We have used an exponential form (equation (5)) for the pitch angle diffusion due to collisions, $D_{\alpha\alpha-\text{collision}}$, the results of which closely resemble the calculations of *Abel and Thorne* [1998] with a sharp rise close to (but slightly outside) the loss cone:

$$D_{\alpha\alpha-\text{collision}} \propto e^{-C_0\alpha} \tag{5}$$

where C_0 is set to reduce $D_{\alpha\alpha-\text{collision}}$ to a negligible value at $\alpha = 15°$ with the result that the overall $< D_{\alpha\alpha} >$, the sum of the pitch angle diffusion due to chorus waves and collisions, is due almost entirely to the chorus waves from just outside the loss cone as presented in Figure 4a. Smoothing out the gradient of phase space density with alpha using the $D_{\alpha\alpha-\text{collision}}$ term is not only more realistic but also has the advantage of preventing overshoot at the loss cone of the cubic spline interpolation method used to swap between the (α, E, L) and (μ, J, L) grids. To remove the sharp change in τ at the loss cone (where τ changes from infinity to 1/4 of the bounce time) is not a trivial calculation. It involves consideration of the degradation of the energy of the electrons as they suffer collisions within a multicomponent atmosphere and is beyond the scope of the current paper.

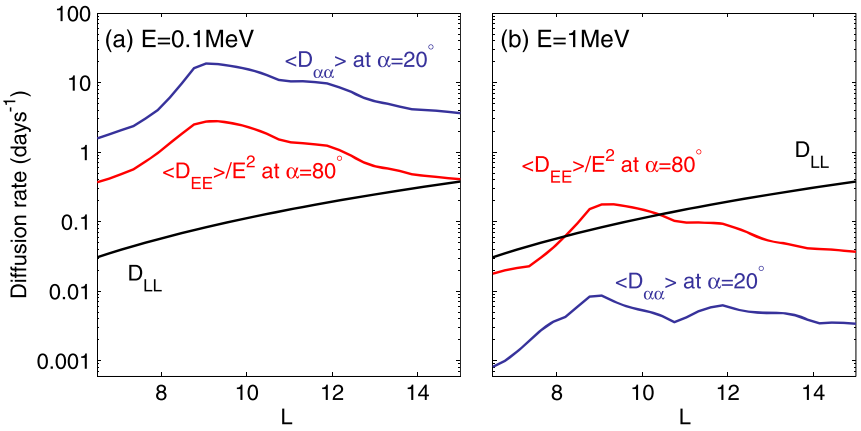

Figure 3. A comparison of diffusion rates from chorus wave particle interactions and radial diffusion for electrons at Jupiter. Bounce-averaged electron pitch angle $< D_{\alpha\alpha} >$, energy $< D_{EE} >$, and radial diffusion D_{LL} are shown for (a) 0.1 MeV and (b) 1.0 MeV.

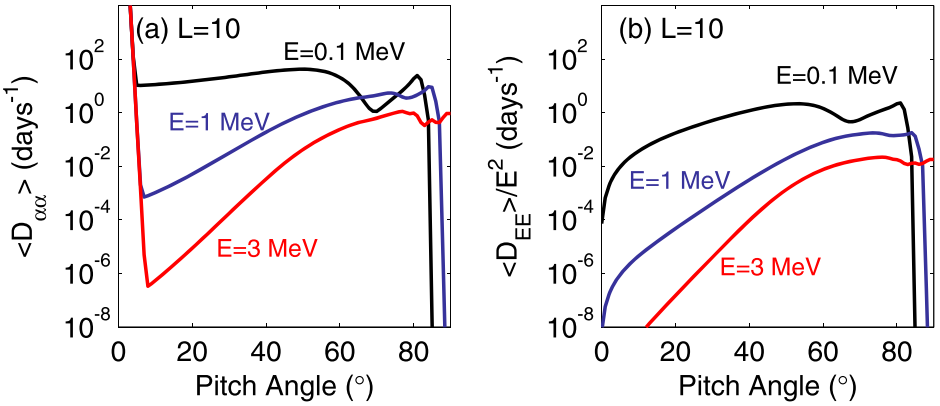

Figure 4. (a) Bounce-averaged pitch angle and (b) energy diffusion rates at $L = 10$ for three selected energies. The large increase in $< D_{\alpha\alpha} >$ at small pitch angles is added to simulate atmospheric collisions.

3. Evolution of Flux From Soft Spectrum

Observations show that injection events can increase the electron flux at energies of tens of keV to hundreds of keV [*Mauk et al.*, 1999; *Louarn et al.*, 2001]. Therefore, we here set the initial condition as a soft energy spectrum associated with an injection event. The injection was set up as a very soft energy spectrum at all values of L in the model, an example of which is shown as the black line ($t = 0$) in Figure 5 for $L = 8.8$ and $L = 13$. However, we maintain the value of the flux at the minimum energy boundary at a constant value over time for the sake of simplicity. We show the effects of changing the initial energy spectrum in the discussion section.

Figure 5 shows how the energy spectra at $L = 8.8$ and $L = 13$ evolve over 100 days due to diffusion by chorus waves alone. There is a very rapid initial response in both cases driven by a combination of large $< D_{EE} >$ at low electron energies and the large gradient of phase space density with energy, followed by a gradually slowing rate of increase in flux at the higher energies. Overlaid on both panels is the electron flux from the GIRE model. Within 9 days the flux at $L = 8.8$ and $E = 3$ MeV has reached the levels observed at Jupiter; at $L = 13$ this takes closer to 100 days. If the simulation is allowed to run for even longer times, the flux at the highest energies is also increased to close to the GIRE values. Although the rate of pitch angle diffusion is larger than the energy diffusion rate at the lower energies, the steep gradient of phase space density with energy drives the rapid increase in flux before the electrons are scattered into the loss cone.

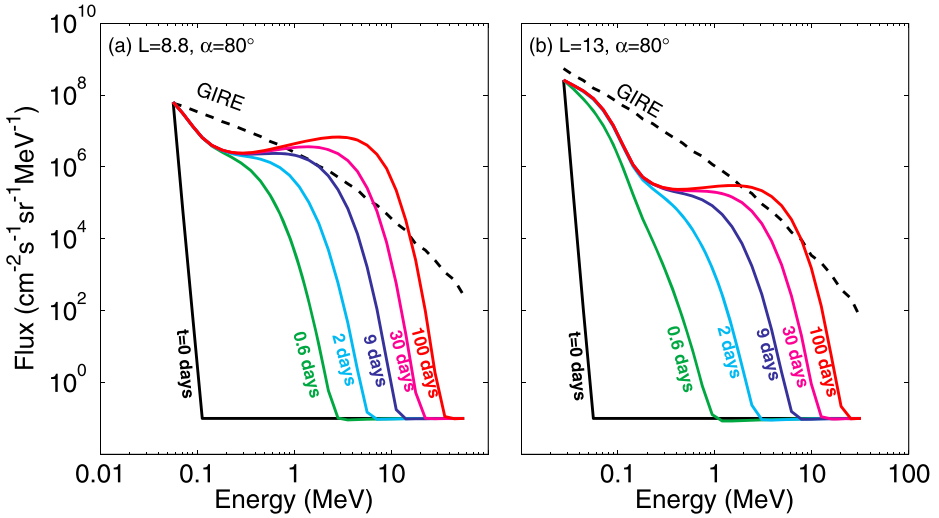

Figure 5. Evolution of energy spectrum over time due to chorus wave acceleration at (left) $L = 8.8$ and (right) $L = 13.0$. No radial diffusion is included. The electron flux from the GIRE model is shown as the dashed black line.

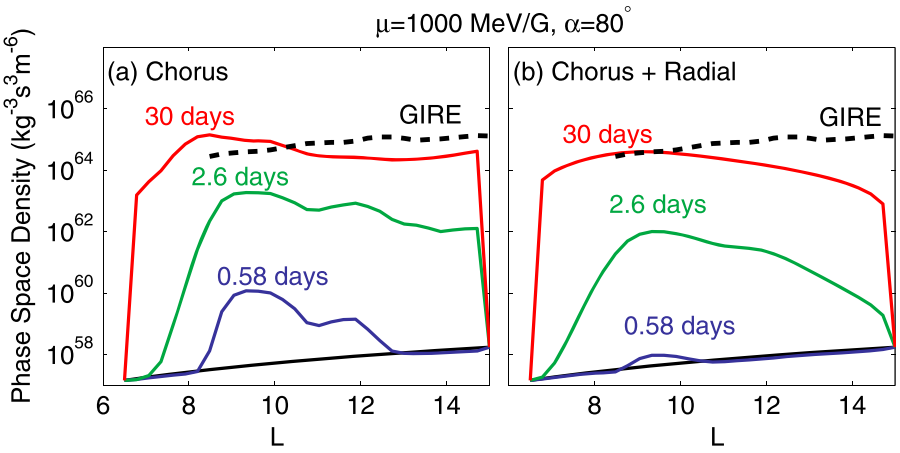

Figure 6. Evolution of phase space density at a constant μ of 1000 MeV/G and $\alpha = 80°$ versus L over time for (a) chorus only and (b) chorus waves and radial diffusion.

Figure 6 shows that over a period of 30 days the phase space density at constant μ increases by a factor of 10^6 or more over the range from $L = 6.5$ to 15 from the very low starting value. When both chorus and radial diffusion are included together (Figure 6b) radial diffusion smooths out the increase in flux generated by chorus. However, the increase in flux is still more than 5 orders of magnitude, indicating that wave acceleration is the dominant process. The rapid increase in flux peaks between $L = 8$ and 10 leading to a peak in electron phase space density at this location which will cause outward radial diffusion for $L \gtrsim 9$.

Figure 7 shows that simulations for radial diffusion alone ("D_{LL}," red line) show only a very gentle increase in phase space density. Radial diffusion alone would never reach the increases seen in the simulations involving chorus unless there was a much larger flux at the outer boundary. We have also included in Figure 7 the results of running the BAS model at Jupiter with no losses (magenta line). Omitting the losses results in a flux that is an order of magnitude higher than the GIRE model at $L = 6$ to 8 in Figure 7a for μ =100 MeV/G and greater than an order of magnitude for the majority of the L in the simulation for μ = 1000 MeV/G (Figure 7b).

Figure 8 shows how the flux at different L values changes with time under three different model scenarios for electrons of 1 MeV and pitch angle of 80°. The radiation belt forms from the soft spectrum with an initial peak near $L = 8$ where the chorus wave intensity peaks. However, for chorus-related and radial diffusion (Figure 8b) the peak in flux lies at slightly lower L, indicating the importance of radial diffusion in

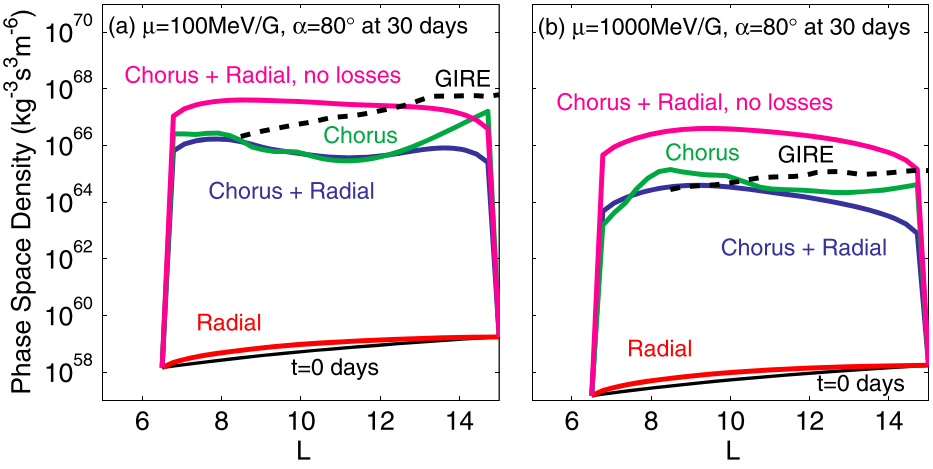

Figure 7. A comparison of phase space density at (a) μ = 100 MeV/G and (b) μ = 1000 MeV/G for chorus only (green), radial diffusion only (red), chorus and radial diffusion (blue), and chorus and radial diffusion with no losses (magenta). The GIRE empirical values are shown as the dashed black line for reference.

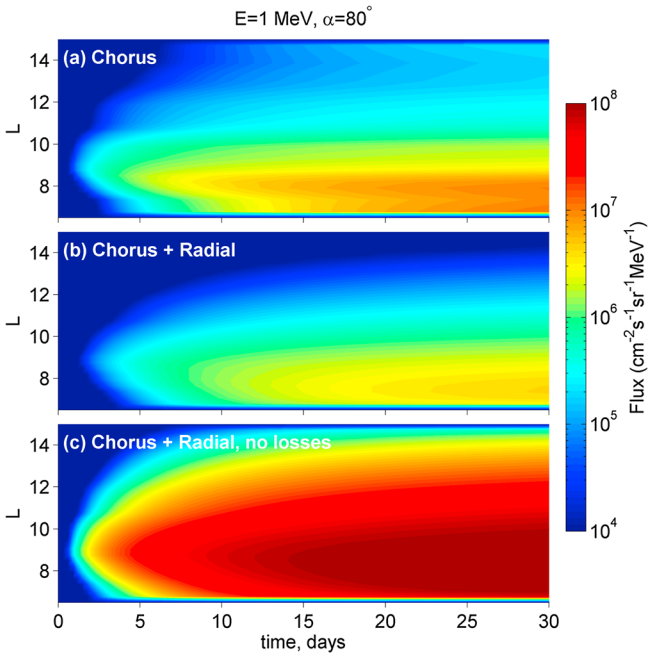

Figure 8. Evolution of flux at 1 MeV and $\alpha = 80°$ for (a) chorus waves only, (b) chorus and radial diffusion, and (c) chorus and radial diffusion with no losses.

redistributing the high-energy particles. Figure 8c demonstrates that the flux could be much higher if there were no scattering into the loss cone and thus losses are very important in calculating the overall growth of the radiation belt.

4. Discussion

We have shown that chorus waves which are known to exist at Jupiter (and could be triggered by the type of injections seen by *Mauk et al.* [1999]) can cause dramatic acceleration of electrons.

The initial conditions in our simulations were set up specifically to test the idea that the radiation belt could be formed by wave acceleration from an initial soft spectrum. In reality injections will come and go with varying profiles in energy, flux, and time. These variations can be investigated by varying individual parameters in the simulation boundary conditions. First, it is important to understand the sensitivity of the results to the softness of the starting energy spectrum. Figure 9 shows three simulations on the same figure with different starting conditions (black, blue, and red) and the resulting spectrum after 30 days. The results are so similar that they cannot easily be distinguished after 30 days (note the black crosses under the red and blue lines). This demonstrates that the softness of the starting spectrum has very limited impact on the resulting spectrum.

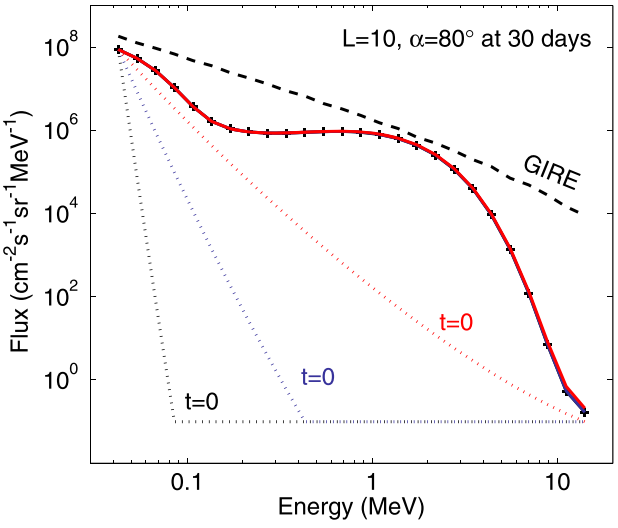

Figure 9. Simulations for three different initial electron spectra at $t = 0$ (black, blue, and red). All three model runs overlay each other after 30 days.

Figure 10 shows the sensitivity to the value of the flux at the minimum energy boundary. When the initial flux at the low-energy boundary was increased by a

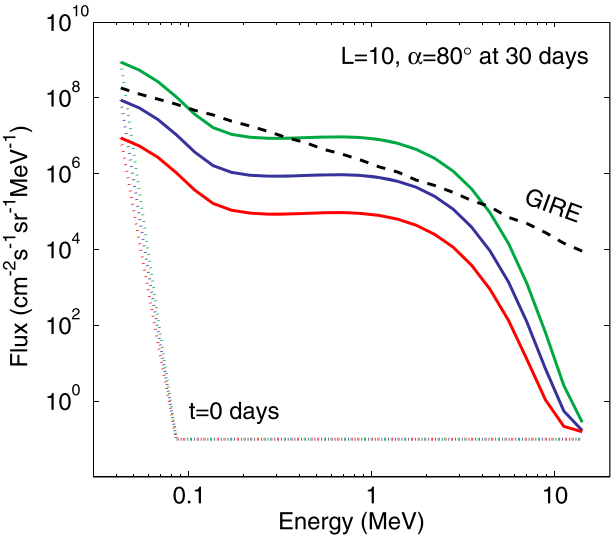

Figure 10. A comparison showing the sensitivity of the simulations to the magnitude of the flux at the minimum energy boundary after 30 days. Each colored line corresponds to a different model run: low flux at minimum energy (red), flux at minimum energy set using the approximation to the GIRE spectrum (blue), and high flux at minimum energy (green). The GIRE spectrum is overlaid for reference as the dashed black.

factor of 10 (green line) the resulting flux after 30 days was significantly increased over a range of energies, up to several MeV. Conversely, reducing the flux by a factor of 10 (red line) reduced the flux up to energies of several MeV. Thus, the results are more sensitive to the low-energy flux than to the hardness of the spectrum. However, the overall shape of the spectrum after 30 days remains very similar regardless of the value of the flux at the low-energy boundary.

Figure 11 shows how the simulation depends on the location of the minimum energy boundary in energy. These spectra were taken from chorus only runs and show how the flux at the very highest energies does not depend on the minimum energy when run for 30 days. As in Figure 10 the value of the flux at the minimum energy boundary is still very important.

We have run simulations (without radial diffusion) where we vary the value of the flux at minimum energy, $J_{E\mathrm{min}}$ with time by a factor of 10 in different patterns (constant on/off, "storm"—constant on/off followed by a wait of 2.5 days and a random pattern, all with the on period being 1 h). The storm pattern of injections is based on the statistics and data presented in *Mauk et al.* [1999], where the characteristic time of a dispersed injection is 1 h and the injections appear to occur in bunches of storm-like activity which recur on approximately a 3 day period. The constant injections and random injection scenarios were used to investigate the effects of other injection timings. If the chorus wave power is assumed constant during these "injections," then the simulation output always lies between those from the lowest and highest values of $J_{E\mathrm{min}}$. Thus, the result of varying the flux at minimum energy over time is an energy spectrum between a minimum and maximum value. If, however, we increase the wave power associated with an injection, then the results are always above those for the lowest value of $J_{E\mathrm{min}}$ but can rise substantially higher than the "maximum" line. These simulations using a time-dependent $J_{E\mathrm{min}}$ also showed that each subsequent injection builds upon the change in flux of the previous injection.

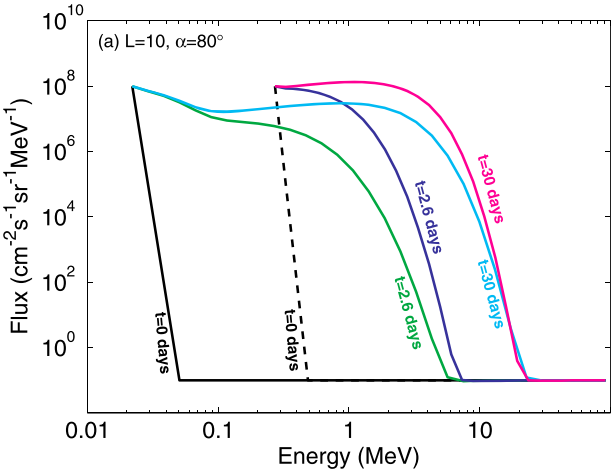

Figure 11. Simulations for two different values of the minimum energy with results shown at 2.6 and 30 days. The simulation with E_{min} = 20 keV is shown in green and cyan that with E_{min} = 250 keV in dark blue and magenta.

Figure 12 shows an example of one of these simulations run using only chorus waves and storm-like injection periodicity. During this simulation the power spectral density of the wave magnetic field is increased by a factor of 10 for each injection by multiplying both $< D_{\alpha\alpha} >$ and $< D_{EE} >$ by 10 (see *Glauert and Horne* [2005], for the dependence of the diffusion rates on the wave power). This extra wave

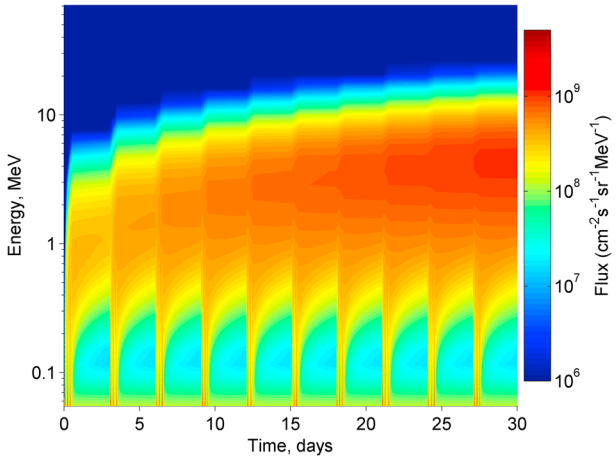

Figure 12. The changing energy spectrum over time for a simulation of storm-like injections using only chorus waves. Both the flux at minimum energy and square of the wave power are increased by a factor of 10 during an injection with the wave power decaying exponentially afterward with a decay time of 1 h. The injection periodicity is on/off for 1 h each for 12 h, then no injections for 2.5 days.

power above the base level then exponentially decays with a timescale of 1 h after the injection finishes. This conservative set of conditions is based on the strength and decay of chorus waves at the Earth [*Meredith et al.*, 2000, Figure 5]. Figure 12 shows that the burst of injection activity leads to a rapid increase in the flux at lower energies which is then accelerated to higher energies more gradually, thus building up the outer radiation belt. This building-up effect was more pronounced the closer together in time the injections occurred but was present in all three of our injection scenarios with or without a change in the wave power during an injection, and independent of the initial value of J_{Emin}. These results depend on the minimum energy boundary being set in the region of tens of keV to a few hundred keV where the diffusion rates calculated from the chorus waves are very rapid. In the lower-energy range we have modeled, which is where the injections are observed, the timing of the injections and the rate of diffusion in energy are such that the effects of one injection can be built upon by the next.

The energy range of interchange events such as the one in *Thorne et al.* [1997] are also suitable to create the same effect although the events are thought to be much shorter than the characteristic 1 h of the *Mauk et al.* [1999] injections. However, since the effects of chorus waves on injections of electrons in this energy range are cumulative, it is highly likely that a combination of interchange events and storm-like injections combine to create the outer radiation belt.

A question we have not yet addressed is what an injection might do to the gradient of phase space density with L. In our simulations, the diffusion due to chorus waves creates a large-scale negative gradient in phase space density from approximately $L = 9$ outward. This suggests that there is a distance beyond which radial diffusion does not contribute to the inner radiation belt and acts as a loss process to transport high-energy electrons away from the Jupiter. A similar situation has been observed at the Earth [*Turner et al.*, 2013].

As at the Earth, there are many wave types with different effects on the electron population at Jupiter. We have focused this paper on whistler mode chorus because it has been shown to cause electron acceleration at the Earth [*Horne et al.*, 2005; *Summers et al.*, 1998; *Chen et al.*, 2007] and Jupiter [*Horne et al.*, 2008; *Woodfield et al.*, 2013]. *Menietti et al.* [2012] show examples of chorus, ECH (electron cyclotron harmonic), and Z mode waves at Jupiter and Saturn. A future survey should look at the power in all of these waves, and the results can be translated into a more rounded picture of the acceleration and losses due to Doppler-shifted cyclotron resonance interactions with electrons at Jupiter.

The latitudinal distribution of chorus wave power is important in determining the effectiveness of the acceleration at different electron energies [*Shprits et al.*, 2012]. *Woodfield et al.* [2013] demonstrated that increasing the wave power at higher latitudes results in the peak of the flux moving to higher energies due to the increases in the rate of pitch angle diffusion at lower energies. Thus, if the chorus waves are more powerful at magnetic latitudes greater than 10° we would still expect the electron flux to increase by a factor of 10^6, but the peak in the energy spectrum would be shifted to higher energies. The flux increases at the very highest energies (> 20 MeV) are not affected by changes in the latitude distribution of the chorus waves [see *Woodfield et al.*, 2013, Figure 4].

The simulations with and without losses neatly encompass the GIRE empirical model of the fluxes at Jupiter (Figure 7). The GIRE phase space density in Figures 6 and 7 shows a decrease from larger to smaller L which

is not reproduced in our results. There are several possible reasons for this. First, the edges of the simulation in L are tied to very low values; this pulls the values of the phase space density close to the edges toward these very low values, particularly where the influence of the chorus waves is weakest at the maximum L boundary. Second, we have neglected some sources of loss in our model, such as the presence of Hiss waves which are known to cause electron losses at the Earth [*Meredith et al.*, 2007] and the presence of more oblique whistler mode chorus which may exist at Jupiter [*Tao et al.*, 2011] and have been found at the Earth [*Artemyev et al.*, 2013] and shown to cause stronger losses [*Mourenas et al.*, 2012] particularly at smaller L.

Including the cross diffusion terms into equation (1) may inhibit the electron acceleration at low pitch angles [*Tao et al.*, 2009]; however, we would still expect the flux at high pitch angles to increase as the effect of cross terms is much less at large pitch angles. It is likely that the inclusion of the cross terms will result in a very anisotropic distribution of electrons and including them in the radiation belt model is the subject of future work.

It is important to point out that the formula we have used for the radial diffusion, although based in theory, has been fixed empirically using Jovian synchrotron radiation [*de Pater and Goertz*, 1994]. It is highly likely that this estimate of D_0 and potentially also the value of n is contaminated in some form by effects from the pitch angle and energy diffusion that we now know to be present at Jupiter. The same would be true of other estimates of the radial diffusion that use the decrease in energetic particles caused by moons [e.g., *Simpson and McKibben*, 1976; *Thomsen et al.*, 1977].

In this study we have neglected the effects of the moon Europa which orbits at 9.4 R_J. As discussed in *Santos-Costa and Bourdarie* [2001] for the inner moons (Metis, Adrastea, Amalthea, and Thebe), a moon orbiting in approximately the rotational equatorial plane at Jupiter will absorb particles with a pitch angle less than approximately 70° due to the offset of the magnetic and rotational axes of the planet. However, particles with larger pitch angles have a much greater opportunity to diffuse across the orbit of the moon since there are periods during Europa's 3.6 day orbit when they will magnetically mirror close to the equator without encountering the moon. By presenting the results for $\alpha = 80°$ we can reasonably neglect the presence of Europa. It is also important to note that since local acceleration due to waves either side of the moon will continue, it is only the radial diffusion of electrons across the orbit of the moon that is affected by the absorption.

Sicard and Bourdarie [2004] suggest that Europa acts as an absorber of particles in a manner similar to the innermost moons of Jupiter. They reached this conclusion based on the similarity of the boundary condition they used at $L = 9.5$ which most effectively recreated the observed synchrotron radiation at low L values. Their boundary conditions were generated by iterating to find a best fit to spacecraft data near $L = 9.5$ and the synchrotron patterns generated by their model very close to Jupiter [see *Sicard and Bourdarie*, 2004, Figure 14]. *Sicard and Bourdarie* [2004] compared their best fit boundary condition at $L = 9.5$ with the energy spectrum generated by setting the boundary at $L = 15$ and treating Europa as an absorbing moon as shown by *Paranicas et al.* [2000]. The latter showed a sharp resonance at 30 MeV compared to the best fit spectrum at $L = 9.5$ which shows a much wider bump noticeably lower in energy than the 30 MeV resonance. *Sicard and Bourdarie* [2004] suggested this mismatch was due to problems extending the assumptions of the Salammbô model beyond $L = 10$. It is very interesting to note that the shape of the boundary condition *Sicard and Bourdarie* [2004] used at $L = 9.5$ which so successfully recreates the synchrotron emissions near the planet resembles very closely the shape of the flux generated by chorus waves in our simulation (cf. *Sicard and Bourdarie* [2004, Figure 3] at $\alpha = 80°$ with our Figure 5]. There is the same peak in the flux between 1 and 10 MeV with a trough at lower energies.

The other moon within the range of L values we have used in our model is Ganymede; however, this is right at the outer edge of the modeled region (at 14.97 R_J) where we have set the boundary to a very low value which would override any and all effects of the presence of Ganymede in these simulations.

5. Conclusions

In this paper we have presented the first simulations of radiation belts at Jupiter which combine both diffusion due to cyclotron resonant interactions between waves and electrons and radial diffusion of electrons. We have demonstrated that whistler mode chorus waves are capable of increasing the flux of an initial very

soft spectrum by 6 orders of magnitude at energies of a few MeV within 30 days if the flux at the minimum energy is sustained.

We have shown that the softness of the initial spectrum is not important; however, the energy range of the injection and the flux in that energy range is important. If the injections are in the energy range that has been observed by *Mauk et al.* [1999], then the effects of the chorus waves build on each previous injection since the timescales involved in the diffusion and the injections are comparable. This cumulative effect would also be true for the shorter-duration interchange events since these are also in the necessary energy range [*Thorne et al.*, 1997].

The effect of radial diffusion on the simulations is to smooth out variations in phase space density created by the rapid flux increase caused by the chorus waves and to transport electrons inward inside $L \sim 9$ and outward beyond it due to the peak in phase space density caused by the waves.

We conclude that cyclotron resonant wave-particle interactions outside of the moon Io could provide the source population for the Jovian radiation belts as suggested by *Horne et al.* [2008].

Acknowledgments

E.E.W., R.B.H., and S.A.G. are funded through STFC grant ST/I001727/1. R.B.H. and S.A.G. are funded in the UK by NERC. J.D.M. is funded by NASA grant NNX11AM36G. Y.Y.S. is funded by NASA grant 443869-YS-22262. Data used in this paper, where not already publicly available, will be stored at the BAS Polar Data Centre and can be accessed by contacting the corresponding author. The authors wish to thank F. Bagenal for the plasma density model and H. B. Garrett and B. Mauk for electron flux data.

M. Balikhin thanks David Shklyar and an anonymous reviewer for their assistance in evaluating this paper.

References

Abel, B., and R. M. Thorne (1998), Electron scattering loss in Earth's inner magnetosphere: 1. Dominant physical processes, *J. Geophys. Res.*, *103*(A2), 2385–2396, doi:10.1029/97JA02919.

Albert, J. M. (2010), Diffusion by one wave and by many waves, *J. Geophys. Res.*, *115*, A00F05, doi:10.1029/2009JA014732.

Albert, J. M., N. P. Meredith, and R. B. Horne (2009), Three-dimensional diffusion simulation of outer radiation belt electrons during the 9 October 1990 magnetic storm, *J. Geophys. Res.*, *114*, A09214, doi:10.1029/2009JA014336.

Artemyev, A. V., O. V. Agapitov, D. Mourenas, V. Krasnoselskikh, and L. M. Zelenyi (2013), Storm-induced energization of radiation belt electrons: Effect of wave obliquity, *Geophys. Res. Lett.*, *40*, 4138–4143, doi:10.1002/grl.50837.

Bagenal, F. (1994), Empirical-model of the Io plasma Torus—Voyager measurements, *J. Geophys. Res.*, *99*(A6), 11,043–11,062, doi:10.1029/93JA02908.

Berge, G. L., and S. Gulkis (1976), Earth-based radio observations of Jupiter: Millimeter to meter wavelengths, in *Jupiter*, edited by T. Gehrels, pp. 621–692, Univ. of Arizona Press, Tucson.

Bolton, S. J., et al. (2002), Ultra-relativistic electrons in Jupiter's radiation belts, *Nature*, *415*(6875), 987–991, doi:10.1038/415987a.

Brautigam, D., and J. Albert (2000), Radial diffusion analysis of outer radiation belt electrons during the October 9, 1990, magnetic storm, *J. Geophys. Res.*, *105*(A1), 291–309, doi:10.1029/1999JA900344.

Brice, N. M., and T. R. McDonough (1973), Jupiter's radiation belts, *Icarus*, *18*, 206–219.

Chen, Y., G. D. Reeves, and R. H. W. Friedel (2007), The energization of relativistic electrons in the outer Van Allen radiation belt, *Nat. Phys.*, *3*(9), 614–617, doi:10.1038/nphys655.

de Pater, I., and D. E. Dunn (2003), VLA observations of Jupiter's synchrotron radiation at 15 and 22 GHz, *Icarus*, *163*(2), 449–455, doi:10.1016/S0019-1035(03)00068-X.

de Pater, I., and C. K. Goertz (1990), Radial diffusion models of energetic electrons and Jupiter's synchrotron radiation: I. Steady-state solution, *J. Geophys. Res.*, *95*(A1), 39–50, doi:10.1029/JA095iA01p00039.

de Pater, I., and C. K. Goertz (1994), Radial diffusion models of energetic electrons and Jupiter's synchrotron radiation: II. Time variability, *J. Geophys. Res.*, *99*(A2), 2271–2287, doi:10.1029/93JA02097.

de Pater, I., et al. (2003), Jupiter's radio spectrum from 74 MHz up to 8 GHz, *Icarus*, *163*(2), 434–448, doi:10.1016/S0019-1035(03)00067-8.

Fok, M.-C., R. B. Horne, N. P. Meredith, and S. A. Glauert (2008), Radiation belt environment model: Application to space weather nowcasting, *J. Geophys. Res.*, *113*, A03S08, doi:10.1029/2007JA012558.

Garrett, H. B., I. Jun, J. M. Ratliff, R. W. Evans, G. A. Clough, and R. W. McEntire (2003), *Galileo Interim Radiation Electron (GIRE) Model*, JPL Publication 03-006, The Jet Propulsion Laboratory, Calif. Inst. of Technol., Pasadena, Calif.

Glauert, S. A., and R. B. Horne (2005), Calculation of pitch angle and energy diffusion coefficients with the PADIE code, *J. Geophys. Res.*, *110*, A04206, doi:10.1029/2004JA010851.

Glauert, S. A., R. B. Horne, and N. P. Meredith (2014), Three dimensional electron radiation belt simulations using the BAS Radiation Belt Model with new diffusion models for chorus, plasmaspheric hiss and lightning-generated whistlers, *J. Geophys. Res. Space Physics*, *119*, 268–289, doi:10.1002/2013JA019281.

Horne, R. B. (1989), Path-integrated growth of electrostatic waves: The generation of terrestrial myriametric radiation, *J. Geophys. Res.*, *94*(A7), 8895–8909, doi:10.1029/JA094iA07p08895.

Horne, R. B., R. M. Thorne, N. P. Meredith, and R. R. Anderson (2003), Diffuse auroral electron scattering by electron cyclotron harmonic and whistler mode waves during an isolated substorm, *J. Geophys. Res.*, *108*(A7), 1290, doi:10.1029/2002JA009736.

Horne, R. B., et al. (2005), Wave acceleration of electrons in the Van Allen radiation belts, *Nature*, *437*(7056), 227–230, doi:10.1038/nature03939.

Horne, R. B., R. M. Thorne, S. A. Glauert, J. D. Menietti, Y. Y. Shprits, and D. A. Gurnett (2008), Gyro-resonant electron acceleration at Jupiter, *Nat. Phys.*, *4*(4), 301–304, doi:10.1038/nphys897.

Li, W., R. M. Thorne, V. Angelopoulos, J. W. Bonnell, J. P. McFadden, C. W. Carlson, O. LeContel, A. Roux, K. H. Glassmeier, and H. U. Auster (2009), Evaluation of whistler-mode chorus intensification on the nightside during an injection event observed on the THEMIS spacecraft, *J. Geophys. Res.*, *114*, A00C14, doi:10.1029/2008JA013554.

Louarn, P., B. H. Mauk, M. G. Kivelson, W. S. Kurth, A. Roux, C. Zimmer, D. A. Gurnett, and D. J. Williams (2001), A multi-instrument study of a Jovian magnetospheric disturbance, *J. Geophys. Res.*, *106*(A12), 29,883–29,898, doi:10.1029/2001JA900067.

Mauk, B. H., D. J. Williams, R. W. McEntire, K. K. Khurana, and J. G. Roederer (1999), Storm-like dynamics of Jupiter's inner and middle magnetosphere, *J. Geophys. Res.*, *104*(A10), 22,759–22,778, doi:10.1029/1999JA900097.

Menietti, J. D., R. B. Horne, D. A. Gurnett, G. B. Hospodarsky, C. W. Piker, and J. B. Groene (2008), A survey of Galileo plasma wave instrument observations of Jovian whistler-mode chorus, *Ann. Geophys.*, *26*(7), 1819–1828.

Menietti, J. D., Y. Y. Shprits, R. B. Horne, E. E. Woodfield, G. B. Hospodarsky, and D. A. Gurnett (2012), Chorus, ECH, and Z-mode emissions observed at Jupiter and Saturn and possible electron acceleration, *J. Geophys. Res.*, *117*, A12214, doi:10.1029/2012JA018187.

Meredith, N. P., R. B. Horne, S. A. Glauert, and R. R. Anderson (2007), Slot region electron loss timescales due to plasmaspheric hiss and lightning-generated whistlers, *J. Geophys. Res.*, *112*, A08214, doi:10.1029/2007JA012413.

Meredith, N. P., R. B. Horne, A. D. Johnstone, and R. R. Anderson (2000), The temporal evolution of electron distributions and associated wave activity following substorm injections in the inner magnetosphere, *J. Geophys. Res.*, *105*(A6), 12,907–12,917, doi:10.1029/2000JA900010.

Mourenas, D., A. V. Artemyev, J.-F. Ripoll, O. V. Agapitov, and V. V. Krasnoselskikh (2012), Timescales for electron quasi-linear diffusion by parallel and oblique lower-band chorus waves, *J. Geophys. Res.*, *117*, A06234, doi:10.1029/2012JA017717.

Nunn, D., Y. Omura, H. Matsumoto, I. Nagano, and S. Yagitani (1997), The numerical simulation of VLF chorus and discrete emissions observed on the Geotail satellite using a Vlasov code, *J. Geophys. Res.*, *102*(A12), 27,083–27,097, doi:10.1029/97JA02518.

Omura, Y., M. Hikishima, Y. Katoh, D. Summers, and S. Yagitani (2009), Nonlinear mechanisms of lower-band and upper-band VLF chorus emissions in the magnetosphere, *J. Geophys. Res.*, *114*, A07217, doi:10.1029/2009JA014206.

Paranicas, C., R. W. McEntire, A. F. Cheng, A. Lagg, and D. J. Williams (2000), Energetic charged particles near Europa, *J. Geophys. Res.*, *105*(A7), 16,005–16,015, doi:10.1029/1999JA000350.

Russell, C. T., S. Georgilas, B. H. Mauk, and D. J. Williams (2004), Io as the trigger of energetic electron disturbances in the inner Jovian magnetosphere, *Adv. Space Res.*, *34*(11), 2242–2246, doi:10.1016/j.asr.2003.09.065.

Santos-Costa, D., and S. A. Bourdarie (2001), Modeling the inner Jovian electron radiation belt including non-equatorial particles, *Planet. Space Sci.*, *49*, 303–312, doi:10.1016/S0032-0633(00)00151-3.

Sault, R. J., T. Oosterloo, G. A. Dulk, and Y. Leblanc (1997), The first three-dimensional reconstruction of a celestial object at radio wavelengths: Jupiter's radiation belts, *Astron. Astrophys.*, *324*(3), 1190–1196.

Schulz, M., and L. J. Lanzerotti (1974), *Particle Diffusion in the Radiation Belts*, Physics and Chemistry in Space, Springer-Verlag, New York.

Shprits, Y. Y., L. Chen, and R. M. Thorne (2009a), Simulations of pitch angle scattering of relativistic electrons with MLT-dependent diffusion coefficients, *J. Geophys. Res.*, *114*, A03219, doi:10.1029/2008JA013695.

Shprits, Y. Y., D. Subbotin, and B. Ni (2009b), Evolution of electron fluxes in the outer radiation belt computed with the VERB code, *J. Geophys. Res.*, *114*, A11209, doi:10.1029/2008JA013784.

Shprits, Y. Y., J. D. Menietti, X. Gu, K. C. Kim, and R. B. Horne (2012), Gyroresonant interactions between the radiation belt electrons and whistler mode chorus waves in the radiation environments of Earth, Jupiter, and Saturn: A comparative study, *J. Geophys. Res.*, *117*, A11216, doi:10.1029/2012JA018031.

Sicard, A., and S. Bourdarie (2004), Physical Electron Belt Model from Jupiter's surface to the orbit of Europa, *J. Geophys. Res.*, *109*, A02216, doi:10.1029/2003JA010203.

Simpson, J. A., and R. B. McKibben (1976), Dynamics of the Jovian magnetosphere and energetic particle radiation, in *Jupiter*, edited by T. Gehrels, pp. 738–766, Univ. of Arizona Press, Tucson, Ariz.

Su, Z., F. Xiao, H. Zheng, and S. Wang (2010), STEERB: A three-dimensional code for storm-time evolution of electron radiation belt, *J. Geophys. Res.*, *115*, A09208, doi:10.1029/2009JA015210.

Summers, D., R. M. Thorne, and F. L. Xiao (1998), Relativistic theory of wave-particle resonant diffusion with application to electron acceleration in the magnetosphere, *J. Geophys. Res.*, *103*(A9), 20,487–20,500, doi:10.1029/98JA01740.

Tao, X., J. M. Albert, and A. A. Chan (2009), Numerical modeling of multidimensional diffusion in the radiation belts using layer methods, *J. Geophys. Res.*, *114*, A02215, doi:10.1029/2008JA013826.

Tao, X., J. Bortnik, J. M. Albert, and R. M. Thorne (2012), Comparison of bounce-averaged quasi-linear diffusion coefficients for parallel propagating whistler mode waves with test particle simulations, *J. Geophys. Res.*, *117*, A10205, doi:10.1029/2012JA017931.

Tao, X., R. M. Thorne, R. B. Horne, B. Ni, J. D. Menietti, Y. Y. Shprits, and D. A. Gurnett (2011), Importance of plasma injection events for energization of relativistic electrons in the Jovian magnetosphere, *J. Geophys. Res.*, *116*, A01206, doi:10.1029/2010JA016108.

Thomsen, M. F., C. K. Goertz, and J. A. Van Allen (1977), A determination of the L dependence of the radial diffusion coefficient for protons in Jupiter's inner magnetosphere, *J. Geophys. Res.*, *82*(25), 3655–3658, doi:10.1029/JA082i025p03655.

Thorne, R. M., T. P. Armstrong, S. Stone, D. J. Williams, R. W. McEntire, S. J. Bolton, D. A. Gurnett, and M. G. Kivelson (1997), Galileo evidence for rapid interchange transport in the Io torus, *Geophys. Res. Lett.*, *24*(17), 2131–2134, doi:10.1029/97GL01788.

Tomás, A., J. Woch, N. Krupp, A. Lagg, K. H. Glassmeier, M. K. Dougherty, and P. G. Hanlon (2004), Changes of the energetic particles characteristics in the inner part of the Jovian magnetosphere: A topological study, *Planet. Space Sci.*, *52*(5-6), 491–498, doi:10.1016/j.pss.2003.06.011.

Trakhtengerts, V. (1999), A generation mechanism for chorus emission, *Ann. Geophys.*, *17*(1), 95–100, doi:10.1007/s005850050739.

Turner, D. L., V. Angelopoulos, W. Li, M. D. Hartinger, M. Usanova, I. R. Mann, J. Bortnik, and Y. Shprits (2013), On the storm-time evolution of relativistic electron phase space density in Earth's outer radiation belt, *J. Geophys. Res. Space Physics*, *118*(5), 2196–2212, doi:10.1002/jgra.50151.

Varotsou, A., D. Boscher, S. Bourdarie, R. Horne, S. Glauert, and N. Meredith (2005), Simulation of the outer radiation belt electrons near geosynchronous orbit including both radial diffusion and resonant interaction with whistler-mode chorus waves, *Geophys. Res. Lett.*, *32*, L19106, doi:10.1029/2005GL023282.

Varotsou, A., D. Boscher, S. Bourdarie, R. B. Horne, N. P. Meredith, S. A. Glauert, and R. H. Friedel (2008), Three-dimensional test simulations of the outer radiation belt electron dynamics including electron-chorus resonant interactions, *J. Geophys. Res.*, *113*, A12212, doi:10.1029/2007JA012862.

Wang, K., S. Bolton, S. Gulkis, and S. Levin (2002), Atmospheric loss of energetic electrons in the Jovian synchrotron zone, *Planet. Space Sci.*, *50*(3), 277–285, doi:10.1016/S0032-0633(01)00129-5.

Woodfield, E. E., R. B. Horne, S. A. Glauert, J. D. Menietti, and Y. Y. Shprits (2013), Electron acceleration at Jupiter: Input from cyclotron-resonant interaction with whistler-mode chorus waves, *Ann. Geophys.*, *31*(10), 1619–1630, doi:10.5194/angeo-31-1619-2013.

Xiao, F., R. M. Thorne, D. A. Gurnett, and D. J. Williams (2003), Whistler-mode excitation and electron scattering during an interchange event near Io, *Geophys. Res. Lett.*, *30*(14), 1749, doi:10.1029/2003GL017123.